Available online at www.eccomasproceedia.org
Eccomas Proceedia COMPDYN (2023) 2618-2627

ECCOMAS
Proceedia

COMPDYN 2023
9th ECCOMAS Thematic Conference on
Computational Methods in Structural Dynamics and Earthquake Engineering
M. Papadrakakis, M. Fragiadakis (eds.)
Athens, Greece, 12-14 June 2023

IN-PLANE RESPONSE OF A MODULAR RETROFIT SYSTEM FOR URM WALLS USING DEM

N. Damiani[1,2*], M.J. DeJong[3], L. Albanesi[4], G. Magenes[2], A. Penna[2] and P. Morandi[4]

[1] University School for Advanced Studies IUSS Pavia
Piazza della Vittoria, 15, 27100 Pavia, Italy
*Corresponding author, e-mail: nicolo.damiani@iusspavia.it

[2] Department of Civil Engineering and Architecture (DICAr), University of Pavia
Via Ferrata 3, 27100 Pavia, Italy
e-mail: {guido.magenes, andrea.penna}@unipv.it

[3] Department of Civil and Environmental Engineering, University of California, Berkeley
760 Davis Hall, Berkeley, CA 94720, United States
e-mail: dejong@berkeley.edu

[4] European Centre for Training and Research in Earthquake Engineering (EUCENTRE)
Via Ferrata 1, 27100 Pavia, Italy
e-mail: {luca.albanesi, paolo.morandi}@eucentre.it

Abstract

Experimental in-plane quasi-static cyclic tests were performed on unreinforced masonry piers to investigate the effectiveness of an innovative retrofit solution. The retrofit consists of modular steel frames fastened to the external surface of masonry walls. Notwithstanding the promising results obtained, they inevitably refer to the specific details of the tested specimens. Advanced and validated numerical models might extend the experimental outcomes enabling a comprehensive study on the retrofit effectiveness. In this paper, numerical models based on the Distinct Element Method are employed to simulate the lateral response of unreinforced and retrofitted masonry piers. All mechanism typical of the in-plane failure of masonry members are included in the models, while a new methodology to account for the contribution of retrofit frames is presented. Numerical outcomes revealed a good prediction in terms of lateral stiffness, lateral strength, and damage pattern for unreinforced and strengthened specimens, enabling the use of the developed models for a parametric analysis to extensively study the behavior of strengthened piers as well as to optimize retrofit details.

Keywords: Numerical Modelling, Distinct Element Method, Framed Retrofit System, Unreinforced Masonry, In-Plane Lateral Response.

ISSN:2623-3347
Peer-review under responsibility of the organizing committee of COMPDYN 2023.
doi: 10.7712/120123.10588.20683

1 INTRODUCTION

The first and essential step to evaluate the effectiveness of newly proposed retrofit solutions in enhancing the seismic response of existing structures is represented by experimental testing. The retrofit system *Resisto 5.9*, designed by the company "Progetto Sisma", underwent an extensive experimental investigation in 2020-2021 at the EUCENTRE and University of Pavia laboratories, Italy. Quasi-static in-plane cyclic tests were performed on unreinforced and retrofitted piers with different masonry typologies typical of Italian existing constructions [1,2]. The retrofit system consists of modular steel frames integrated with thermal insulation coatings, and connected to the masonry external surface. It aims at enhancing the wall in-plane response, but also at improving the connection between orthogonal walls as well as limiting wall out-of-plane overturning. The retrofit was conceived as an integrated solution able to fulfil, in addition to structural aspects, "modern" requirements such as energy-efficiency, light weight, cost-effectiveness, and ease of installation [3–7].

Notwithstanding the promising enhancement of the pier in-plane capacities observed in the dedicated experiments, the achieved results refer to the specific properties of the tested specimens (e.g. masonry material properties, pier aspect ratios, vertical load, retrofit details …). In this regard, reliable and validated numerical models represent a valid option to extend experimental outcomes to achieve a thorough insight into the performance of the investigated retrofit solution. Among the various modelling strategies employed in literature, the Distinct Element Method (DEM) [8], has been demonstrated to be a suitable micro-modelling approach for the simulation of the response of URM structures [9–14]. However, limited applications about the integration of possible strengthening solutions in the same numerical environment have been carried out so far.

In this contribution, distinct element models were developed to simulate the experimentally observed in-plane response of unreinforced and retrofitted masonry piers. The models, built using the software 3DEC [15], are able to account for the several aspects that influence the in-plane response of masonry elements, such as mortar joint opening and dislocation, unit tensile failure and masonry crushing under high-compressive stresses. Note that, of the various masonry typologies tested within the experimental campaign, only one was considered herein, consisting of solid clay bricks and lime mortar assembled in a header bond pattern. Retrofit frames and their connection with the masonry were explicitly modelled using finite elements and nonlinear structural links, as recently proposed by Damiani et al. [16]. Monotonic loading schemes and a dynamic relaxation approach, alongside time, size and mass scaling techniques, were used to reduce the computational effort.

After validating the adopted numerical strategy against the experimental outcomes, the developed models were used to perform additional analyses aimed at further investigating the retrofit effectiveness on the in-plane behavior of masonry walls. The performed analyses included different combinations of overburden loads and retrofit details, such as the connections between retrofit and adjacent floors. It is worth to notice that the parametric study presented in this contribution represents only a preliminary part of a still ongoing extensive numerical exercise that will be object of future publications.

2 DESCRIPTION OF THE ADOPTED NUMERICAL STRATEGY

In the present section, the major aspects of the numerical strategy adopted to replicate the in-plane quasi-static behavior of both unreinforced and strengthened masonry members is provided. Comprehensive details about the adopted assumptions and formulations, as well as a further discussion on the entire set of employed parameters, can be found in [16].

2.1 Unreinforced masonry modelling using DEM

In this work, a simplified micro-modelling strategy based on DEM was employed. According to this approach, masonry units are modelled as rigid or deformable continuum blocks, while zero-thickness nonlinear spring layers provide the connection between units (Figure 1). In case of deformable blocks an internal discretization (or mesh) is required to capture unit deformability. In this work, units were discretized into multiple hexahedral finite-difference regions, formed of two set of five overlapping constant-strain tetrahedral elements [17].

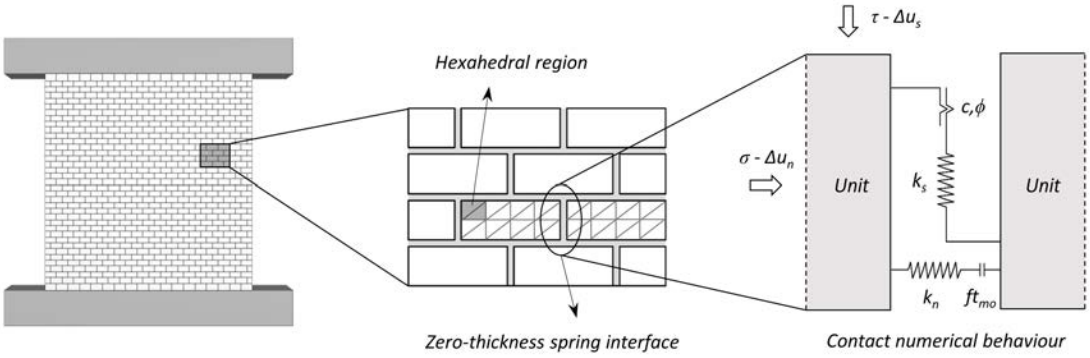

Figure 1: Discretization of masonry according to DEM.

The mechanical properties of unit-mortar interfaces (i.e. normal stiffness k_n, bond tensile strength ft_{mo}, shear stiffness k_s, cohesion c, and friction angle ϕ) were lumped into the zero-thickness interfaces as shown in Figure 1. A Coulomb-slip model was employed to represent the joint (or contact) shear behavior (Figure 2a). In the normal direction joint tensile failure was admitted, while joint compressive limit was not specified (Figure 2b). The normal and shear joint stiffness were evaluated as $k_n = E_{mo}/t_{mo}$ and $k_s = G_{mo}/t_{mo}$ [11,16], where E_{mo} and G_{mo} are the mortar elastic and shear moduli, and t_{mo} is the thickness of mortar joints. The adopted joint constitutive laws account for post-peak softening regimes through the definition of shear (G_s) and tensile (G_{tj}) fracture energies [13].

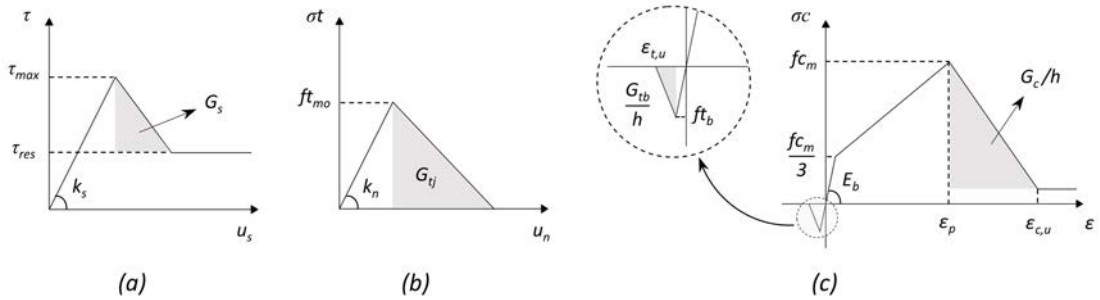

Figure 2: Constitutive laws: joint shear (a) and tensile (b) behavior; (c) block tensile and compressive behavior.

Since no compressive failure was admitted at the unit-mortar interfaces, a Mohr-Coulomb plasticity model was assigned to the blocks to account for both masonry crushing under high-compressive stresses and unit tensile failure (Figure 2c). The compressive behavior was modelled using a linearized version of the Feenstra and De Borst strain-softening model [14]. The model assumes a bi-linear stress-strain relationship up to the peak strain $\varepsilon_p = 4fc_m/3E_b$, where fc_m is the masonry compressive strength and E_b is the unit elastic modulus. After the peak value, the strength linearly decreases until it reaches a small residual value at the ultimate strain $\varepsilon_{c,u} = \varepsilon_p + 3G_c / 2fc_m h$, where G_c is the fracture energy of masonry in compression while h is

the crack bandwidth. The unit tensile behavior was replicated using a linear strain-softening law [16]. After the peak strain, the tensile strength ft_b linearly reduces to zero at the ultimate tensile strain $\varepsilon_{t,u} = 2G_{tb} / ft_b\, h$, where G_{tb} is the tensile fracture energy of the masonry units.

2.2 Retrofit system modelling

The retrofit at issue consists of steel frames connected to the masonry through chemical anchors and to each other through steel bolts [1,2]. The frames include L-shaped border profiles, and horizontal and diagonal bracings made of thin plate sections. Figure 3a summarizes the typical dimensions and components of a retrofit module. Each member was modeled as a one-dimensional beam finite element (FE) with linear elastic behavior. To consider buckling of plate elements, a sinusoidal deformation with a 1-mm amplitude was pre-imposed to each brace at the crossing points of the diagonal braces and mid-length of the horizontal ones [16]. Pre-deformed FE beams are shown as dashed lines in Figure 3b. Rigid links were used to model connections between adjacent steel modules. An elastic modulus of 210 GPa, a Poisson coefficient of 0.30, and a density of 7850 kg/m^3 were assigned to the FE beams.

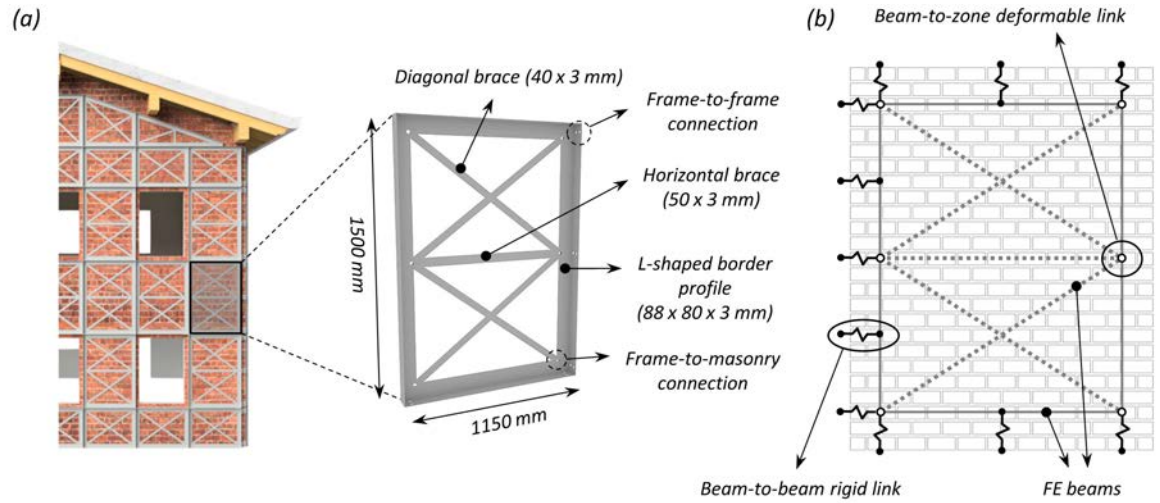

Figure 3: Retrofit system modelling: (a) layout and steel module details; (b) numerical layout.

The connections between the steel frames and masonry were simulated using nonlinear deformable links that connected the FE beams to the blocks. Each link was assigned a shear-yield model for the three translational degrees of freedom, while the rotational ones were left free. The behavior of the links in the two directions in the masonry pier plane (x, z) was determined based on the results of shear tests conducted on retrofit-to-masonry anchors (Figure 4). Likewise, based on the results of extraction tests, a bilinear force-displacement rule was assigned to the links along the pier out-of-plane direction (y) [16].

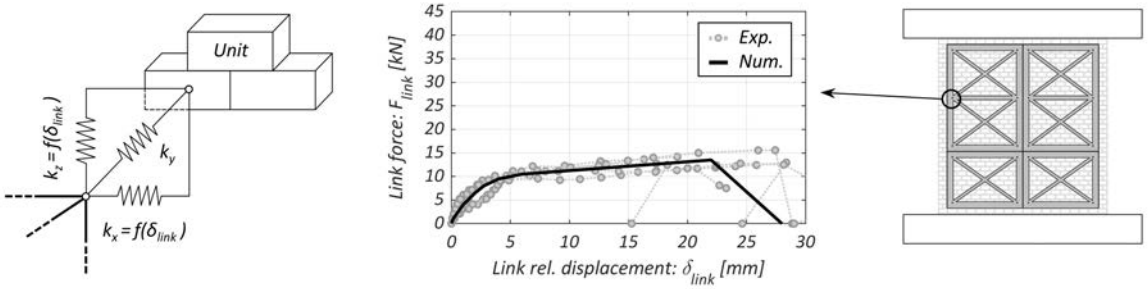

Figure 4: Numerical behavior of retrofit-to-masonry connections.

3 MODEL VALIDATION AGAINTS EXPERIMENTAL DATA

The proposed modelling strategy was verified against the experimental data coming from quasi-static in-plane cyclic tests performed on identical masonry piers in unreinforced (U) and retrofitted (R) conditions. Note that among the tested piers, only one was considered in this contribution. The masonry pier consisted of 120 x 250 x 55 mm clay bricks and 10-mm thick mortar joints (t_{mo}) assembled in a single-wythe header bond pattern, resulting in height H = 2435 mm, length L = 2330 m, and thickness t = 250 mm. Unreinforced and retrofitted counterparts were tested under an overburden stress σ_v = 0.50 MPa and double-curvature boundary conditions. Table 1 summarizes the masonry mechanical properties assigned in the models. Comprehensive details about the values assigned to the different parameters can be found in [16]. Moreover, regarding the experimental retrofit scheme, no connection was considered between the steel frames and the reinforced concrete (RC) top beam and foundation [1,2].

Masonry & Units	E_m [MPa]	fc_m [MPa]	ρ_m [kg/m^3]	E_b [MPa]	ft_b [MPa]	G_c [N/m]	G_{tb} [N/m]
	4265	7.03	1300	7207	1.79	11248	60
Joints	k_n [GPa/m]	k_s [GPa/m]	c [MPa]	ϕ [°]	ft_{mo} [MPa]	G_s [N/m]	G_{tj} [N/m]
	126	50	0.15	31.38	0.05	50	10

Table 1: Masonry material properties assigned in the models [16].

3DEC is based on a dynamic time-integration algorithm that solves the equations of motion by an explicit finite-difference method. In this work, quasi-static phenomena were solved by damping the equations of motion to quickly reach a force equilibrium state by employing a numerical servo-mechanism, called adaptive global damping [11,15,18]. Size, density and time-scaling techniques were also employed to obtain a compromise between the accuracy of results and the computational expense. Units were discretized according to the strategy recently proposed by Damiani et al. [16], resulting in 8x1x4 and 2x1x1 meshes for the "corner" and "central" pier regions, respectively. Note that the notation employed above indicates the number of hexahedral regions employed along the unit length, thickness and height (Figure 1).

The reinforced-concrete (RC) top beam and foundations were modeled as blocks with a linear elastic behavior (E = 40 GPa), while the application of the overburden load was simulated by assigning an equivalent density to the RC top beam. Pier lateral displacements were induced by incrementally applying multi-stepped velocity histories to the RC top beam. The velocity was increased gradually, leading to a displacement of 1 mm in 0.135 sec. After each 1-mm displacement, an equilibrating phase occurred [11]. Note that in this contribution, only monotonic loading schemes were employed. However, for the complete set of numerical results, including the simulation of pier cyclic responses and of the other masonry typologies tested during the same experimental campaign, the reader is referred to [16].

Figure 5 compares the experimental and numerical outcomes in terms of force-drift ratio (or displacement) envelopes and failure modes. Drift ratios (θ) were computed dividing the imposed lateral displacement by the pier height. Notwithstanding the underestimation of the pier peak strengths, numerical models resulted in a good prediction of the pier experimental responses. In particular, the retrofit was able to increase the pier drift-ratio capacity, countering the opening of cracked mortar joints and delaying the strength degradation exhibited by the unreinforced counterpart, as observed in the experiments [1,2]. Note that in the displayed numerical crack patters, joint relative displacements were reported with the same order of magnitude to clearly appreciate the retrofit influence.

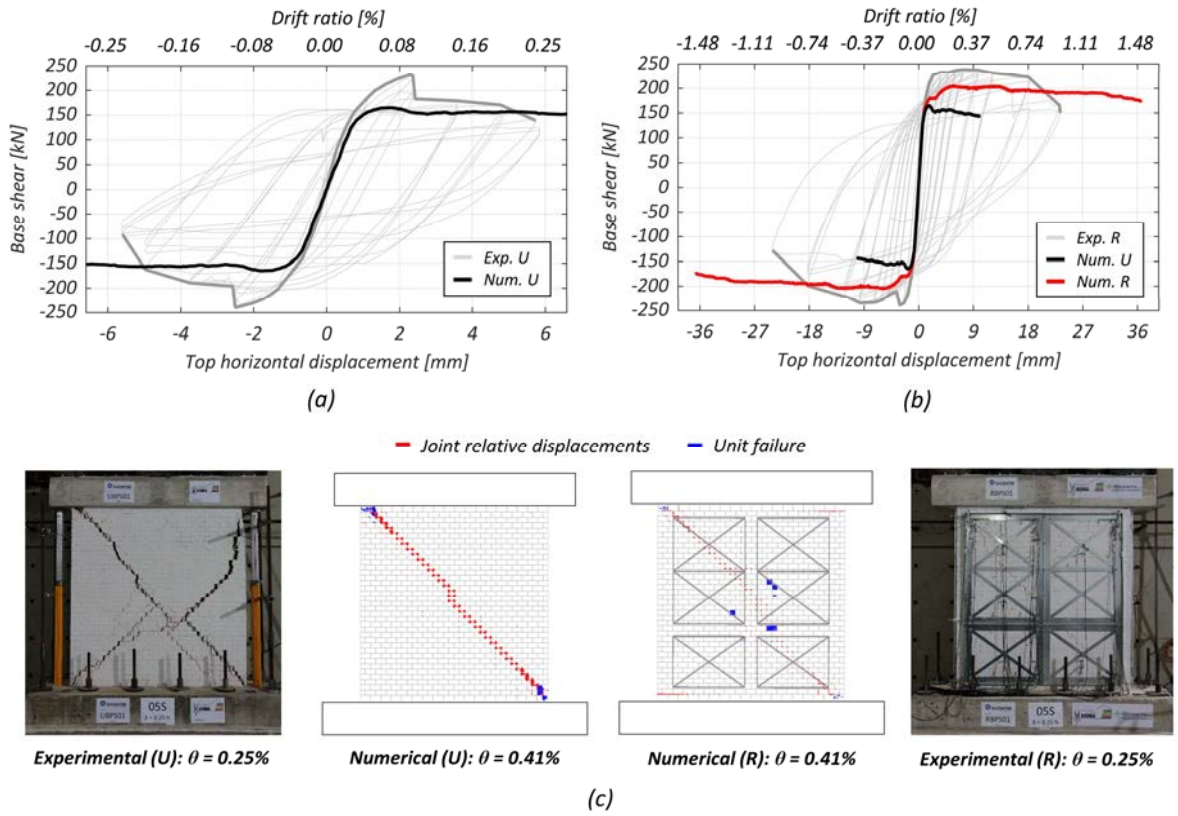

Figure 5: Experimental vs numerical outcomes: (a) unreinforced pier force-displacement envelopes; (b) retrofitted pier force-displacement envelopes; (c) damage patterns.

In the experiments, the unreinforced and retrofitted piers achieved maximum drift ratios of 0.25% and 0.97%, respectively. Looking at the numerical outcomes, the bare and retrofitted piers exhibited ultimate drift-ratio capacities (θ_u) of respectively 0.41% and 1.50%, evaluated at a strength drop of around the 20% of the maximum strength. Although numerical models overestimated the experimental drift-ratio capacities (likely due to the monotonic loading and underestimation of the peak strength), the retrofit effectiveness was adequately captured. Indeed, the retrofit system increased the numerical drift-ratio capacity of the unreinforced pier by a factor of 3.66, closely matching the experimental value of 3.88.

4 PARAMETRIC ANALYSIS

In this section, the proposed numerical strategy was employed to perform additional analyses varying some fundamental factors to further assess the retrofit performance, extending the available experimental outcomes. Two main aspects were investigated, i.e., the level overburden stress (σ_v) and the effects of retrofit-to-floors connections. Note that only the experimental boundary conditions and pier aspect ratio (H/L = 1.05) and were considered herein.

Besides the experimental overburden σ_v = 0.50 MPa, two additional values of 0.30 MPa and 0.80 MPa were investigated. The considered values of σ_v corresponded to axial load ratios (σ_v / fc_m) of respectively 4%, 7%, and 11%. While the reference experiments did not involve connecting the retrofit to the top and bottom RC elements representing floors or foundations (Figure 5), steel frames are typically applied to the entire facade of a masonry building in real applications to ensure the continuity of the intervention along the building's height (Figure 3a). To investigate the effects of connections to adjacent floors on the retrofitted pier responses, additional FE beams (representing L-shaped border profiles, see Figure 3) were defined to

extend the retrofit up to the top and bottom RC elements, as shown in Figure 6. The results of experimental shear tests performed on retrofit-to-RC anchors [1] were employed to define the nonlinear rule assigned to the newly defined links (Figure 6).

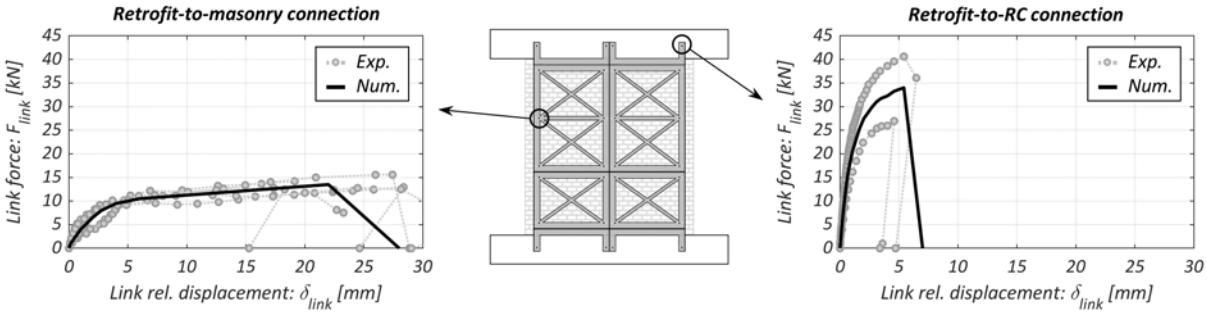

Figure 6: Connected retrofit layout and numerical behavior of structural links.

Monotonic pushover analyses were then performed for each of the 9 considered configurations. During the analyses, three relevant parameters were monitored, i.e., the maximum base shear (V_{max}), the associated drift ratio (θ_{Vmax}), and the ultimate drift ratio (θ_u) assumed at a strength drop of around $0.2V_{max}$. Figure 7 reports the set of performed analyses. Herein, asterisk markers indicate the attainment of the maximum lateral force, while pier ultimate conditions are identified by circle markers. The monitored quantities obtained for unreinforced piers (U) and retrofitted piers with non-connected (R) and connected (RCC) retrofit layout, are summarized quantitatively in Table 2. Herein, the effectiveness of the considered retrofit schemes is also reported and quantified as the ratio between the parameters obtained for retrofitted and unreinforced piers (identified as R/U, RRC/U and RRC/R).

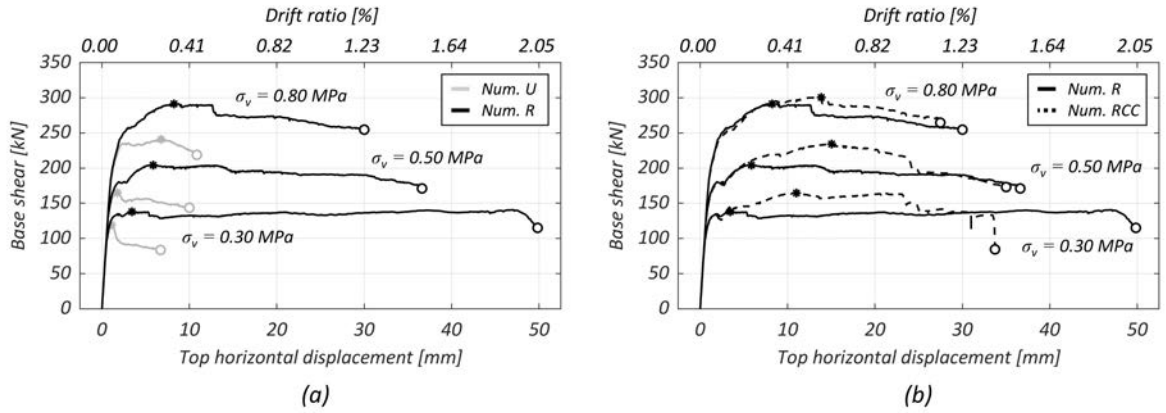

Figure 7: Numerical outcomes: (a) unreinforced vs retrofitted pier pushover curves; (b) influence of retrofit-to-floors connections.

Overall, the retrofit did not alter the initial stiffness and failure mechanism of unreinforced piers, and delayed the joint opening and the strength degradation, in accordance with experimental evidence. Looking first at the results related to the non-connected retrofit scheme reported in Figure 7a, an appreciable improvement of the URM pier responses was observed, especially in terms of drift-ratio capacities. In this regards, it is possible to observe how retrofit performance benefits associated with θ_{Vmax} and θ_u essentially decreased as the overburden load increased (Table 2). Small improvements of around 20% were also observed in terms of V_{max}, although they could be biased by the peak strength underestimation exhibited by the unreinforced pier models (Figure 5a).

In Figure 7b the pushover curves obtained for the non-connected (R) and connected (RCC) layouts of the retrofit are compared to highlight the influence of the retrofit-to-floors connections, not directly addressed in the reference experimental campaign. Compared to the non-connected configuration, the connection of the retrofit to the top and bottom RC elements resulted in greater benefits in terms of V_{max} and θ_{Vmax} for all considered levels of σ_v, while, on the other hand, it led to an overall reduction of the ultimate deformation capacity as denoted by the RCC/R ratios reported in Table 2.

σ_v [MPa]	Parameter	Pier configuration			R/U [-]	RCC/U [-]	RCC/R [-]
		U	R	RCC			
0.30	V_{max} [kN]	119	138	165	1.16	1.39	1.20
	θ_{Vmax} [%]	0.05	0.14	0.45	2.80	9.00	3.21
	θ_u [%]	0.28	2.05	1.38	7.32	4.93	0.67
0.50	V_{max} [kN]	165	204	234	1.24	1.42	1.15
	θ_{Vmax} [%]	0.07	0.24	0.62	3.43	8.86	2.58
	θ_u [%]	0.41	1.5	1.44	3.66	3.51	0.96
0.80	V_{max} [kN]	241	291	300	1.21	1.24	1.03
	θ_{Vmax} [%]	0.28	0.34	0.57	1.21	2.04	1.68
	θ_u [%]	0.45	1.23	1.13	2.73	2.51	0.92

Table 2: Summary of numerical results and retrofit performance benefits.

Overall, the performed numerical analysis confirmed the retrofit effectiveness observed in the experimental tests, revealing a substantial improvement of the fundamental parameters of the in-plane response of masonry piers, at least for the addressed masonry typology and pier aspect ratio. Among the monitored quantities, the ultimate drift-ratio capacity represents the most relevant parameter for practical design applications of this strengthening solution. The retrofit increased the ultimate drift-ratio capacity of URM piers by a factor ranging from 7.32 to 2.73 in case of a non-connected scheme, while by a slightly lower factor ranging from 4.93 to 2.51 for a connected layout.

CONCLUSIONS

In this paper, a numerical study was conducted to investigate the performance of a modular steel-based retrofit system on the in-plane lateral response of masonry piers. The retrofit solution involved modular steel frames connected to the masonry. Numerical models based on the Distinct Element Method were built and validated using the experimental results from quasi-static in-plane cyclic tests performed on unreinforced and retrofitted piers. The developed models were able to simulate all the possible failure mechanisms of masonry members, and to explicitly include the contribution of the investigated retrofit solution.

One of the different masonry typologies tested during the experimental campaign was considered in the study, consisting of solid clay bricks arranged in a header bond pattern. The in-plane response of monotonically loaded masonry piers in both unreinforced and retrofitted configurations was investigated, assessing in particular the effect of the level of overburden load and the connection of retrofit frames to the adjacent floors, not addressed in the reference experiments.

Although the numerical analyses presented in this contribution were associated with a specific masonry typology and a unique pier aspect ratio, they showed that the studied retrofit

was able to counter the development of damage in both mortar joints and units. This delayed the progressive strength reduction and significantly improved the drift-ratio capacities of all the tested piers, confirming the experimental results. The retrofit performance decreased as the vertical overburden increased, while the connection of the retrofit frames to the adjacent floors led to smaller retrofit benefits especially in terms of ultimate drift-ratio capacity, if compared to the non-connected retrofit layout tested within the experimental campaign.

An ongoing extensive parametric study, object of future publications, will include additional combinations of other fundamental variables herein not addressed, such as different pier aspect ratios and masonry typologies, aiming at achieving a comprehensive insight into retrofit performance benefits.

ACKNOWLEDGEMENTS

The experimental and numerical research activities described in this paper were performed at the EUCENTRE Foundation and were funded by Progetto Sisma s.r.l.. The study of the modelling approach proposed for unreinforced masonry specimens was partially supported and funded by DPC-ReLUIS Work Package 10 Subtask 10.1 (2022–2024) "Modelli di capacità locali e globali per la definizione degli stati limite, definiti in funzione del metodo di analisi". The received financial and technical support is gratefully acknowledged. Thanks go also to F. Graziotti whose valuable advice was essential to the study.

REFERENCES

[1] C.F. Manzini, L. Albanesi, P. Morandi, Studio del comportamento sismico di murature portanti con rivestimento esterno modulare in acciaio. *Research report EUC054/2021-EUC088/2021U*, 2022 (in Italian). https://progettosisma.it/2_sperimentazione_eucentre/

[2] L. Albanesi, C.F. Manzini, P. Morandi, In-plane cyclic tests of URM walls strengthened with an innovative external steel modular framing system. In *Progresses in European Earthquake Engineering and Seismology*, *3rd European Conference on Earthquake Engineering and Seismology*, Bucharest, Romania, 2022.

[3] D.A. Pohoryles, C. Maduta, D.A. Bournas, L.A. Kouris, Energy performance of existing residential buildings in Europe: A novel approach combining energy with seismic retrofitting. *Energy and Buildings* **223**, 110024, 2020.

[4] M. Busselli, D. Cassel, A. Prada, I. Giongo, Timber Based Integrated Techniques to Improve Energy Efficiency and Seismic Behaviour of Existing Masonry Buildings. *Sustainability* **13(18)**, 10379, 2021.

[5] M.R. Valluzzi, E. Saler, A. Vignato, M. Salvalaggio, G. Croatto, G. Dorigatti, T. Umberto, Nested Buildings: An Innovative Strategy for the Integrated Seismic and Energy Retrofit of Existing Masonry Buildings with CLT Panels. *Sustainability* **13**, 1188, 2021.

[6] G. Guerrini, N. Damiani, M. Miglietta, F. Graziotti, Cyclic response of masonry piers retrofitted with timber frames and boards. *Proceedings of the Institution of Civil Engineers - Structures and Buildings* **174(5)**, 372-388, 2021.

[7] M. Miglietta, N. Damiani, N, G. Guerrini, F. Graziotti, Full-scale shake-table tests on two unreinforced masonry cavity-wall buildings: effect of an innovative timber retrofit, *Bulletin of Earthquake Engineering* **19**, 2561-2596, 2021.

[8] P.A. Cundall, A Computer Model for Simulating Progressive Large Scale Movements in Blocky Rock Systems. In *Proceedings of the Symposium of the International Society of Rock Mechanics*, Nancy, France, 1971.

[9] J.V. Lemos, Discrete element modeling of masonry structures. *International Journal of Architectural Heritage* **1(2)**, 190-213, 2007.

[10] J.V. Lemos, Discrete element modeling of the seismic behavior of masonry construction. *Buildings* **9(2)**, 43, 2019.

[11] D. Malomo, M.J. DeJong, A. Penna, Distinct element modelling of the in-plane cyclic response of URM walls subjected to shear-compression. *Earthquake Engineering & Structural Dynamics* **48(12)**, 1322-1344, 2019.

[12] D. Malomo, M.J. DeJong, A. Penna, Influence of Bond Pattern on the in-plane behavior of URM Piers. *International Journal of Architectural Heritage* **15(10)**, 1492-511, 2019.

[13] B. Pulatsu, E. Erdogmus, P.B. Lourenço, J.V. Lemos, K. Tuncay, Simulation of the in-plane structural behavior of unreinforced masonry walls and buildings using DEM. *Structures* **27**, 2274-2287, 2020.

[14] D. Malomo, M.J. DeJong, A Macro-Distinct Element Model (M-DEM) for simulating the in-plane cyclic behavior of URM structures. *Engineering Structures* **227**, 111428, 2021.

[15] Itasca, *3 Dimensional Distinct Element Code (3DEC). Theory and Background, 7th edition*, Itasca Consulting Group, 2019.

[16] N. Damiani, M.J. DeJong, L. Albanesi, A. Penna, P. Morandi, Distinct element modelling of the in-plane response of a steel-framed retrofit solution for URM structures. *Earthquake Engineering and Structural Dynamics,* 2023. doi: 10.1002/eqe.3910.

[17] J. Marti, P. Cundall, Mixed discretization procedure for accurate modelling of plastic collapse. *International Journal for Numerical and Analytical Methods in Geomechanics* **6(1)**, 129-139, 1982.

[18] J.R.H. Otter, Dynamic relaxation compared with other iterative finite difference methods, *Nuclear Engineering Design* **3(1)**, 183-185, 1966.